SLAC-PUB-140
September 1965

STREAMER CHAMBER DEVELOPMENT

F. Bulos, A. Boyarski, R. Diebold, A. Odian, B. Richter, F. Villa

Stanford Linear Accelerator Center

Stanford University

Stanford, California

ABSTRACT

Some properties of the streamer chamber will be presented. Special attention is given to the practical use of large volume chambers as particle detectors. In particular, the following problems are discussed:

a) Pulsing of large volume chambers

b) Reducing the rather long memory of the chamber by suitable quenching

c) Amplification of the light output by the use of image intensifiers with large photocathode area.

All measurements have been made on straight tracks from particles of various energy. Scatter and curvature fitting as well as ionization measurement (using gap length technique) will be presented.

(Invited paper at the Fifth International Conference on High-Energy Accelerators, Frascati, Italy, September 9-16, 1965)

STREAMER CHAMBER DEVELOPMENT

F. Bulos, A. Boyarski, R. Diebold, A. Odian, B. Richter, and F. Villa

Stanford Linear Accelerator Center,
Stanford University, Stanford,
California, U.S.A.

The increased interest in spark chambers over the last few years has lead to the addition of two new types: the wide gap spark chamber[1-5] and the wide gap streamer chamber[4,6-13]. The essential difference in the method of operation of these two types is that in the wide gap spark chamber the parameters (magnitude and length) of the high voltage pulse allow a spark to develop while in the streamer chamber the discharge is arrested at an early stage by suitable pulse shaping. The particle tracks in the two chambers are distinctively different. The track in the wide gap spark chamber appears as a continuous spark (discharge) independent of the direction from which it is viewed. In the streamer chamber, however, the track looks like a series of dots (similar to bubble chamber tracks) when viewed through transparent electrodes along the electric field. Perpendicular to the field the track appears as a series of streaks (streamers) whose length depends on the parameters of the high voltage pulse (see figures for illustration). A comparison of the most important properties of the two chambers appears in Table 1.

It is easily seen from Table 1 that the streamer chamber is equal or superior to the spark chamber in the first four properties. In five the excessive memory of the chamber and the diffusion of tracks with time are undesirable for use at particle accelerators with long beam spill, and in experiments where a continuous background exists (for example, storage rings).

In such cases it is desirable to reduce the memory of the chamber. Clearing fields commonly used in narrow gap spark chambers are ineffective here, because the clearing time for wide gap chambers would amount to several μsec. Workers in this field have relied on proper gas mixing (poisoning) for memory reduction. For the streamer chamber one desires a gas which reduces the memory to < 5 μsec without causing any deterioration in the precious light output. We have investigated several gases.

Diffusion and chamber memory study

1. Diffusion

A chamber 30 x 30 x 12 cm^3 was used. The chamber was filled with a mixture of Ne-He (90%-10%) and cosmic ray tracks were photographed with variable delays of the high voltage pulse ranging from 0.15 μsec to 200 μsec. Figure 4 is a typical picture which illustrates the diffused character of the track which results from the high voltage pulse delay. Figure 5 shows the dependence of the projected width (σ) of the track on the magnitude of pulse delay t. It is seen that σ has a $\sqrt{t}$ dependence which is what is expected from diffusion theory. Theory gives:

$$\sigma^2 = 4Dt,$$

where D is the diffusion coefficient. We find

$$\sigma^2 \ (cm^2) = 1640 \ t \ (\text{seconds}).$$

Comparing with theory we obtain

$$D = 410 \ cm^2/\text{sec}.$$

The value of D is smaller than the accepted value by more than a factor of five.

2. Memory

Next we investigated the effect of the admixture of several promising gases on the memory reduction. A smaller chamber 15 x 15 x 6 cm^3 was used. To speed up data taking β rays from an Sr^{90} source and the necessary thin counters and windows were used. The following gases were found effective in reducing the chamber memory to < 5 μsec without decreasing the light output appreciably. They appear in increasing order of percentages required:

Freon-12, Ethylene, Methane.

SO_2, though effective in reducing the memory, had undesirable side effects.

Figures 6a,b,c show a detailed study of the effect of a few parts per million admixture of Freon-12 on the memory of chamber and track quality. It is clear that the memory of the chamber can be easily reduced to 1 μsec or less if desired.

Light output

The small light output from streamer chambers remains its most serious drawback (item 5, Table 1). It is well known that a small f-number (wide lens aperture) leads to a small depth of field. Present experiments in high-energy physics require large volume spark chambers. When large volume streamer chambers are photographed with the necessary small f-number, a serious defocusing results. A point light source at different parts of the chamber appears as a circle of variable diameter as a result of the variable defocusing. Thus, one is forced to seek a compromise focus which gives the lowest upper limit on the size of the point source resulting from possible defocusing. This limit is given by the diameter (d) of the circle of least confusion:

$$d_{space} = \frac{\Delta u}{2Fm}, \quad d_{film} = \frac{\Delta u}{2Fm^2}, \qquad (1)$$

where Δu is the total depth of field, F is the f-number and m is the demagnification.

For example, d_{space} = 5 mm for F = 2, m = 50 and Δu = 1 meter.

In this case a line source of zero width can appear to have 5 mm width in space. This defocusing limits the resolution and track location accuracy. One can compensate for small f-numbers by large demagnification; however, the resolution of film and lenses and maximum precision in film positioning put an upper limit on demagnification (for detailed considerations and figure of merit of film see Appendix A).

Thus, it appears that for practical purposes the defocusing due to small f-numbers required in streamer chamber photography remains the most serious limiting factor on resolution.

There are two obvious approaches to the problem:

a) finding faster films;

b) increasing the light output of the chamber or amplifying the available output artificially (by the use of image intensifiers).

a) Film search

We investigated many of the commercially available films. The method adopted was practical. A chamber 30 x 30 x 12 cm was used. Films were compared in pairs, photographing the same cosmic-ray tracks. The pulse parameters and the experimental conditions were kept the same. Many tracks were photographed and for each film the best developers were used. We list here the best films in order of decreasing speed:

Kodak 2475, Royal X pan and Tri-X, Shell burst and linograph.

Others such as polaroid films (10,000, 3000 ASA) and expanded range films were poorer. Other methods of comparison such as photographing d.c. sources of light (neon bulb, for example) or relying on quoted speed were sometimes misleading. However, the better films always proved to have the following quoted properties: low threshold, and high acuteness. We are in consultation with Kodak for speedy films and have investigated special films which proved to be slightly faster than 2475, although they were most difficult to handle. With proper developing the speed of 2475 is $\approx$ 3000 ASA.

b) Increasing the light output

At first many workers[10] including us hoped that some magic gas or gas mixture would give more light. The result is that pure neon or neon-helium mixture remains the best gas. Other noble gases (helium, for example) give less light, are more difficult to operate. Non-noble gases mixed with neon essentially "poison" the chamber as was mentioned in the investigation of the chamber memory.

However, it was noticed by our Russian colleagues[9] and us that the brightness of the tracks increases somewhat with the increase of electric field. We have investigated the dependence of streamers shape and brightness on the parameters of the high voltage pulse as follows:

Cosmic-ray tracks were photographed on 2475 film with various pulses ranging in width from 5-25 nsec and in amplitude from 10-20 kV/cm. For each pulse the f-number (F) was increased from 1.5 (minimum available)

in steps of 1/4 f-stop up to F = 11, i.e. well past cut-off. For each f-stop at least 10 tracks were photographed. The square of cut-off f-number (i.e. the maximum f-number at which tracks on the average become too faint to be practically useful) was considered to be proportional to the brightness (B) in the streamer view ($\perp$ to the field) and proportional to the total light output in the view along the field. For each pulse the widths of several streamers were measured and the average recorded together with the cut-off f-number. Seven different pulse shapes were investigated. For each pulse shape the data was internally normalized. Each of the following properties: streamer length (L), streamer brightness (B) and total light output (TL) was assumed to follow a power law of the electric field E (kV/cm) and pulse width τ (nsec):

$$(\text{normalized property})_i = E^{x_i} \tau^{y_i}. \qquad (2)$$

For each property L,B,TL a fitting program was used to find the best value of x,y for the seven different E,τ groups. We tabulate the results in Table 2.

Such measurements are difficult because of the unavoidable fluctuation of pulse parameters and possible, though mild, variation of light output with the degree of ionization of particles producing the track[4], which was not controlled in this experiment. However, one can draw very useful information from Table 2:

1) The ratio of the power of E to that of τ is large (4-6) for all the three properties.

2) On investigating the dependence of B on E and τ one has to be careful. Only equal length streamers should be considered. For equal

length streamers Eq. 2 leads to the following relations:

$$\text{(a)} \qquad B \propto E^{x_2 - \frac{x_1 y_2}{y_1}}$$

$$\text{(b)} \qquad B \propto \tau^{y_2 - \frac{y_1 x_2}{x_1}} .$$

Table 2 shows that the power of τ in (b) tends to be negative but consistent with zero. The power of E in (a) = 2.4 ± 0.6. Physically this means that if one increases the electric field and keeps the streamers length constant by reducing the pulse width, the streamers brightness increases very nearly proportional to the square of E. However, if one increases the pulse width and keeps the streamers length constant by reducing the electric field at best the brightness does not change. As an illustration Figs. 7 and 8 show two sets of pictures for two different pulse shapes, each taken with progressively increasing f-numbers.

Similar measurements were made using an image intensifier (see below). The results are in good agreement with the above observations.

3) Within the experimental error the total light (as defined above) is proportional to the product of the streamers brightness and their length.

Use of image intensifiers[11)]

A two-stage tube RCA(C70012) with a 3.5" photocathode and anode has been tried. The nominal gain and resolution of this tube is about 1500 and 25 lines/mm, respectively. Photographs with up to f/11 were taken

with this tube, when the streamer lengths were 5 mm. Figure 9 shows typical photographs with small and large f-numbers for comparison. To photograph with an f-number about 16, we are planning to use a three-stage tube (RCA C70055) with a nominal gain of 50,000.

In practical use the two-stage tube proved to have a resolution at the back face of the tube corresponding to 20 lines/inch in object space for a demagnification of about 25. The over-all system including the back lens and film gave a resolution of 7-10 lines/inch in object space. We believe that this could be improved by using better lenses especially at the back where most of the resolution and light loss occurs.

Comparing the performance of the tube and direct photography for equal length streamers, we find that the practical gain of the tube and lens system = 12.

However, we caution that such tubes have characteristic "S" distortion. Figure 10 shows the reproduction of a quadrant of line grid, precision ruled on a lucite plate and edge illuminated.

It clearly shows that the distortion increases sharply after the 1/2 radius point. Figure 11 gives a measurement of the distortion in a typical tube quadrant as a function of x,y the undistorted coordinates on the back face of the tube. We feel that the usefulness of the tube is limited by the degree to which one can correct for these distortions, which are rather large compared to the degree of precision attained in streamer chambers.

Curvature and scatter measurement

In order to determine the spatial accuracy with which tracks can be located, a study was made on the scatter of streamer dots from the fitted trajectories for particles. Protons with 600 MeV/c momentum

obtained from a target at the Stanford Mark III accelerator were made to pass parallel to the plates of the chamber. No magnetic field was used at the chamber. The delay time of the high voltage pulse was about 0.3 μsec after the passage of the particle. An 80 mm f/2.8 lens was used with a demagnification factor of 20 on the film. Tri-X film was used, and the average streamer lengths were about one centimeter. Track lengths were 24 cm in the chamber.

The coordinates (x,y) of each streamer in the front view (parallel to $\vec{E}$) were measured and punched on cards. A least-squares fit was then made to the points of each track having the form:

$$y = a + bx + \frac{1}{2} cx^2,$$

where a, b and c were varied. All tracks were oriented approximately along the x direction. From the distribution of the residuals:

$$r_i = y_i - (a + bx_i + \frac{1}{2} cx_i^2),$$

the projected scatter of a streamer was determined to be 0.23 mm average for all the tracks.

A comparison can be made between the error in the curvature resulting from the streamer scatter and the actual curvature measurements "c" obtained from a large number of straight tracks. There were an average of 31 points per track, and if we approximate the streamer locations to one of uniform spacing along the track, we can use the curvature error estimates given by Gluckstern[15]. For $\sigma = 0.23$ mm, the curvature error, assuming a purely statistical scatter, is found to be 1.8×10^{-4} cm^{-1}.

Coulomb scattering in Neon at one-atmosphere would produce a curvature error of about 0.6×10^{-4} cm^{-1}. Effects of optical distortions on the curvature were determined by photographing straight wires throughout

the field of view of the streamer tracks. For wire lengths equal to the track lengths, and for equal number of measurements along the wire length, a curvature error of 1.5×10^{-4} cm^{-1} was found. Hence one would expect a curvature distribution for many streamer tracks to be about 2.4×10^{-4} cm^{-1}. The actual distribution of "c" from 80 tracks is shown in Fig. 1. The rms scatter is 3.0×10^{-4} cm^{-1} which is slightly larger than that calculated above.

Using the measured curvature error of 3.0×10^{-4} cm^{-1}, a chamber of 24 cm could observe momenta up to 10 BeV/c if a magnetic field of 10 kG were used, i.e.

$$\frac{\sigma p}{p} \approx \frac{0.06\ p}{BL^2}$$

for p in GeV/c, B in kG and L in meters.

The distribution of scatter from the particle trajectory is shown in Fig. 13 at the 150 nsec delay. It agrees with a normal distribution with a 0.16 mm width. The measurer's setting, as determined by repeatedly measuring the coordinates of one dot, is only 0.05 mm. The streamer dot size in the view along the field was about 1.5 mm diameter.

Gap length distribution

The gap length distribution between adjacent streamers was measured at the shortest delay time. This is shown in Fig. 14. The expected distribution is exponential and the cut-off at about 2.0 mm indicates that approximately 50% of the streamers are prevented from developing by a robbing action between closely spaced streamers.

The exponential region for gap lengths greater than about 4 mm can be used to obtain the correct streamer density if robbing were not present. Thus, we obtain the true mean gap as 2.8 mm and the mean streamer density as 3.6/cm. The number of streamers is a factor of 10 less than would be expected if each ion pair had a mean energy of about 35 eV given by the ionization potential, and produced a streamer.

Some measurements were made on particles with different ionizing power. Dot density measurements were made for minimum ionizing pions (I_{min}) and protons with 2.3 I_{min}. One might expect the number of streamer dots to be proportional to the ionizing power of the passing particle, thus providing a useful tool for dE/dx measurement. A small sample of pion and proton tracks showed promising results but when a larger sample of 40 pion tracks and 80 proton tracks were analyzed, a ratio of streamer density of only 1.2 was found, which is considerably less than 2.3. This may be due to variable operating conditions during the experiment. On the other hand, it might just be due to the increased "robbing" effects in the proton tracks due to their higher streamer density. For a theoretical attempt see Ref. 7.

The number of streamer dots at a delay of a few microseconds was found to be larger by about a factor of two over short delay times. This can be explained by the robbing action of closely adjacent streamers. At longer delay times the average separation between electrons is larger, so that the robbing is less and more streamers become visible. Similar conclusions can be drawn from Fig. 6a.

Brief outline of theory

All the essential features of streamer formation can be found scattered in Refs. 16 and 18. An outline of the theory appears in Refs. 4 and 17. Reference 19 contains a more detailed attempt along the same lines.

Briefly the applied electric field acts on the electrons left behind by the ionizing charged particle. These electrons are accelerated during the voltage pulse. They lose a small energy, ~ m/M, by elastic collisions (m,M are masses of electron and atom, respectively). Thus, they keep gaining energy until they can multiply by ionization. The process is described by the first Townsend coefficient α. N_o electrons accelerated for a distance x multiply to N electrons where

$$N = N_o \, e^{\alpha x}.$$

This process goes on until the space charge field inside the avalanche cancels the external field. The first avalanche thus reaches its critical size. However, in this process photons are emitted from the highly ionized gas in the avalanche. These photons produce further electrons by photoionization. The electrons quickly multiply into secondary avalanches in the intensified electric field made up of the external field and the space charge field just outside the positive and negative tips of the primary avalanche. If the external field persists this mechanism goes on until secondary avalanches connect, leading to a complete discharge involving the electrodes. This discharge is the spark observed in wide gap and narrow gap spark chambers.

A detailed calculation is difficult because it involves uncertain terms such as: which photons are most important and with what efficiency do they produce photoionization? How many visible photons per electron does one expect? The process is, however, inefficient which explains the small light output until a complete breakdown (spark) occurs. But as was noted[4], one does not have to know anything about gaseous discharge to make a working streamer chamber. All one needs is a good-quality well-controlled

pulse to be able to stop the above mechanism at any stage of streamer development required.

Pulsers and chambers

1. Pulsers

For obtaining good-quality tracks in a streamer chamber one requires a high voltage pulse 10-20 kV/cm with a good rise time ($\leq$ 5 nsec) and a fairly short fall time. Pulse tails $\geq$ 50 nsec force an undesirable decrease in the amplitude of total pulse (see above) otherwise they cause breakdowns. In practice, pulse widths $\approx$ 10 nsec give very good tracks.

The simplest method to produce such pulses has been developed and used successfully by both Russian workers[4,9] and ourselves. Figure 15a shows a schematic diagram of such a pulser. A high voltage exponential pulse is generated by a Marx-type generator (MG). The quality of the pulse can be excellent (rise time $\approx$ 2 nsec, and 80-90% of the theoretically expected voltage). One can use such a generator to drive the chamber directly. The pulse width is regulated by adjusting the pressure and spacing of the pressurized shorting gap (ShG). The gap can be placed either before or after the chamber. To prevent pulse jitter the shorting gap should be prepared (triggered) before the arrival of the HV pulse. The best scheme which leads to stable operations is to trigger the gap from the first stages of the generator. Such gaps are highly over-voltaged and work very well for delays within the spark formation time of the gap ($\leq$ 50 nsec). Beyond that they jitter.

Marx generators, however, have an inevitable internal impedance due to resistances and inductances of the generator capacities and leads. Pulse-height loss follows when driving small impedance loads ($<$ 50 Ω).

A modification which avoids this and can be used to gain voltage is the use of resonance charging. Essentially one uses the Marx generator to charge a low inductance capacity c_1 (preferably of the coaxial type) through an inductance (ℓ). The energy is transferred resonantly from the generator to the capacity which can then charge up to a voltage > the output voltage of the generator. A series pressurized gap after the capacity is adjusted (by suitable spacing and pressure) to fire at the peak voltage of the first charging cycle of the capacity. c_1 then becomes the chamber voltage source and, together with the shorting gap, determines the quality and parameters of the pulse. Small chambers act as a capacitive load but large chambers (> 50 cm along pulse travel) begin to show the characteristic of a transmission line. If the chamber is left unterminated the pulse is reflected at the open end of the chamber with the same polarity, thus almost doubling the voltage on the chamber. For chambers 1 m long the total reflection time becomes comparable with pulse widths used. In this case the voltage at different points in the chamber differs in time. Such chambers should be terminated and the additional gain of voltage by reflection is lost.

We have used a ten-stage Marx generator of effective capacity = 300 μμf. A capacity = 120 μμf was charged resonantly through a 1 μh inductance. This pulser gave a voltage pulse up to 250 kV useful at the chamber with a d.c. supply voltage = 26 kV. A slightly modified Marx generator was also constructed capable of generating 800 kV maximum. The principle of the generator is shown schematically in Fig. 15b. As an alternative, single cable pulsers (or cable doublers) can be used to generate square pulses of the desired width but with an amplitude = 1/2

the charging voltage. This loss hurts when very high voltages are desired. In addition, the d.c. voltage insulation and the spark gap switch required become difficult.

An interesting way out is to combine the principle of the Marx generator with the property of a cable. In principle if the capacities in Fig. 15b were replaced with low impedance open-ended cables having an electric length equal to 1/2 the pulse width, and the system properly terminated, one obtains a square pulse of the required width and with an amplitude = 1/2 nV_o, where n = number of cables, V_o = d.c. charging voltage. The total impedance is nz, where z is the impedance of a single cable. We are currently investigating the possibility of constructing a 600 kV, 30 Ω pulser with a pulse width ≈ 10 nsec using the above principle.

2. Chambers

When very large gap chambers are required (> 20 cm), the voltage requirements become difficult. We therefore investigated the possibility of making two gap streamer chambers with a central high voltage electrode and two outside grounded electrodes. All electrodes were made of wire mesh, and special attention was paid to make the two compartments and their connections to the pulse generator electrically identical. The chamber (70 x 70 x (2 x 15) cm) showed excellent tracks of cosmic rays. We are investigating whether any distortions appear in tracks that pass through the central high voltage electrode. In addition to easing the voltage requirement, two compartment chambers are better suited for use in magnetic fields where limited space leads to high voltage shielding problems.

Finally we wish to give some practical observations which might be very useful to the reader.

1. The insulated walls of streamer chambers should be continuous inside the chamber. Breaks in the walls, such as windows, lead to violent breakdowns or distortions. Distortions have also been observed when small dielectric cylinders were introduced inside the chamber[20].

2. Electrodes can be made of metal conducting glass or wire mesh. However, if wire mesh is used it should not be placed inside the chamber. It will always glow undesirably. Mesh electrodes should be separated from the chamber gas by an insulator such as plexiglas.

3. In two-compartment and one-compartment chambers, conductors (other than chamber-generator ground), which are near the high voltage electrode, should not have an electrical connection to the chamber ground otherwise the chambers either stop working completely or show undesirable sparking. Some chambers immediately worked when the common chamber-generator ground was electrically isolated from the metal frame supporting the chamber and generator).

The above observations are easier to explain after they are observed.

Table 1

Comparison between wide gap spark chambers and streamer chambers

		Streamer chamber	Spark chamber
1.	Accuracy of track location and momentum measurement	Excellent	Excellent[2,3,5]
2.	Multiple track efficiency	Excellent. No apparent robbing (Figs. 1 and 2)	Good, but exhibits robbing[5]
3.	Track following capability	Excellent in all directions	Excellent up to an angle 20° with the perpendicular to the electrodes. Slowly deteriorates between 20°-40°. Becomes poor for angles $> 40^{\circ}$. Also track quality suffers
4.	Vertices in the chamber gas, δ rays, etc.	All shown clearly (Fig. 3)	Poor. See Ref. 14 for the best of a few pictures to date
5.	Memory	> 200 μsec. Tracks diffuse in time, Fig. 4b	About 5 μsec with some track deterioration
6.	Light output	Poor. Fast films (ASA > 1000) and small f-numbers (f/2) are needed	Excellent. f/22 is quite adequate

Table 2

Property	x	y
Streamer length L	4.7 ± 0.9	1.16 ± 0.32
Streamer brightness B	2.4 ± 0.6	- 0.09 ± 0.23
Total light TL	5.2 ± 1.0	1.03 ± 0.38

APPENDIX A

Depth of field and figure of merit for films

We use the following easily derivable relations:

1. The illumination of the image $\propto 1/F^2$, where F = lens f-number.
2. The diameter (d) of the circle of least confusion at the film is given by $d = \Delta u/2Fm^2$, where Δu is the total depth of field and m is the demagnification.

Now, for the same f-number and object brightness the degree of darkening of the film is related to the film speed (measured here by the ASA number) as follows:

$$\text{darkening} \propto \text{ASA}. \tag{A1}$$

It follows then from (1) and Eq. (A1) that for a minimum acceptable darkening of the film

$$\frac{1}{F^2} \geq \frac{250}{\text{ASA}} . \tag{A2}$$

For the best over-all spatial resolution one tries to match the resolution of lenses and film, then chooses the demagnification such that the resolution from depth of field (determined by the diameter of the circle of least confusion) also matches. Then:

$$\frac{\Delta u}{2Fm^2} = \frac{1}{S} , \tag{A3}$$

where S is the matched resolution of lenses and film in lines/unit length. But the demagnification is also subject to the condition that the size of image $\geq 1/S$. Therefore for an object of length ℓ:

$$\frac{\ell}{m} \geq \frac{1}{S} . \tag{A4}$$

Equations (A1), (A2) and (A4) give:

$$\Delta u = \frac{2Fm^2}{S} \leq \text{constant} \times \ell^2 \times S \times \sqrt{ASA} \ .$$

For objects of the same brightness and size and the same acceptable darkening of the film, the maximum depth of field is determined by the product of the resolution and $\sqrt{\text{speed}}$ of the film.

Therefore, from the point of view of depth of field, the above product is the figure of merit of the film.

However, for each situation an equation similar to (A2) must always be satisfied independently otherwise the image will not register at all on the film.

REFERENCES

1) S. Fukui and S. Miyamoto, Nuovo Cimento 11, 113 (1959).

2) A.I. Alikhanian, T.L. Asatiani, A.M. Matevosian and R.O. Sharkhatunian, Phys.Letters 4, 295 (1963).

3) A.I. Alikhanian, T.L. Asatiani and E.M. Matevosian, JETP 17, 522 (1963).

4) A.I. Alikhanian, LOEB Lecture Notes, Harvard University (1965).

5) J.P. Garron, D. Grossman and K. Straugh, Rev.Sci.Instr. 36, 264 (1965).

6) V.A. Mikhailov, V.N. Roinishvili and G.E. Chikovani, JETP 19, 561 (1964).

7) G.E. Chikovani, V.N. Roinishvili and V.A. Mikhailov, JETP 19, 833 (1964).

8) B.A. Dolgoshein and B.I. Luchkov, JETP 19, 266L (1964).

9) G.E. Chikovani, V.N. Roinishvili, V.A. Mikhailov and A.K. Javrishvili, Preprint, Institute of Physics of the Academy of Science of GSSR, Tbillisi (1964).

10) B.A. Dolgoshein, B.I. Luchkov and B.U. Rodionov, JETP 19, 1315 (1964).

11) M.M. But-slov, V.I. Komarov and O.V. Savshenko, Nucl.Instr.and Methods 34, 289 (1965).

12) E. Gygi and F. Schneider, CERN 64-30 (351), CERN 63-37 (145).

13) F. Bulos, A. Boyarski, R. Diebold, A. Odian, B. Richter and F. Villa, SLAC-PUB-105, May (1965).

14) R.C. Catura and K.W. Chen, Princeton-Pennsylvania Accelerator Department (PPAD-2137-552) (1965).

15) R.L. Gluckstern, Nucl.Instr.and Methods 24, 381 (1963).

16) LOEB, Basic processes of gaseous electronics.

17) F. Bulos, SLAC TN-64-73, September (1964).

18) J.M. Meek and J.D. Craigs, Electrical breakdown of gases, Oxford Clarendon Press (1953).

19) J.K. Wright, Proc.Roy.Soc. 280A, 24 (1963).

20) M.E. Davon, V.E. Kazerov, S.A. Krilov, Lebedev Institute of Physics (Preprint) (1965).

FIG. 1--Multiple tracks, electrons, view along $\vec{E}$ f/2.8

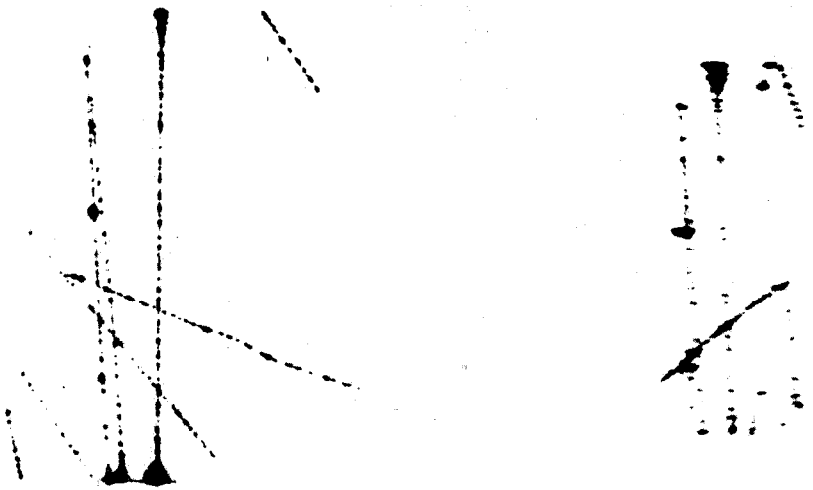

FIG. 2--Cosmic ray shower
90° stereo
f/1.5

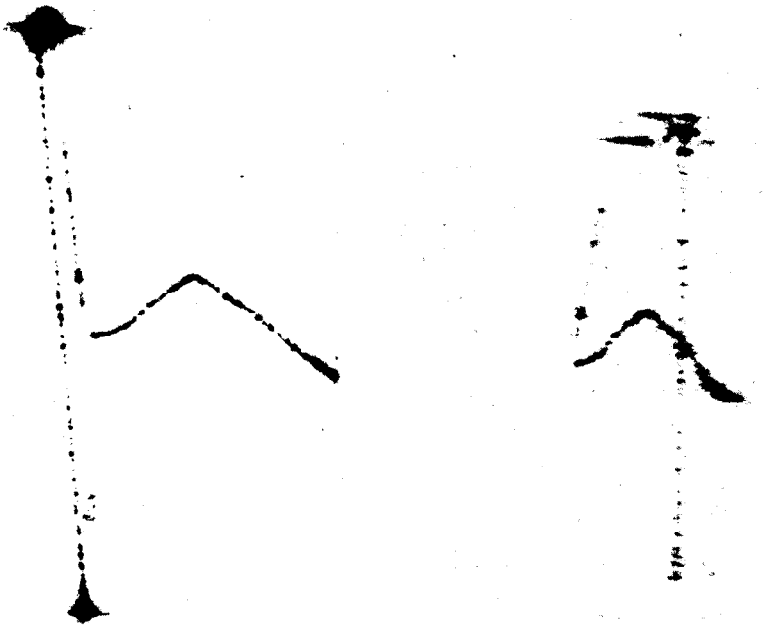

FIG. 3--Streamer track. 90° stereo. Scattering vertices appear very clearly both at the chamber wall and in the gas.

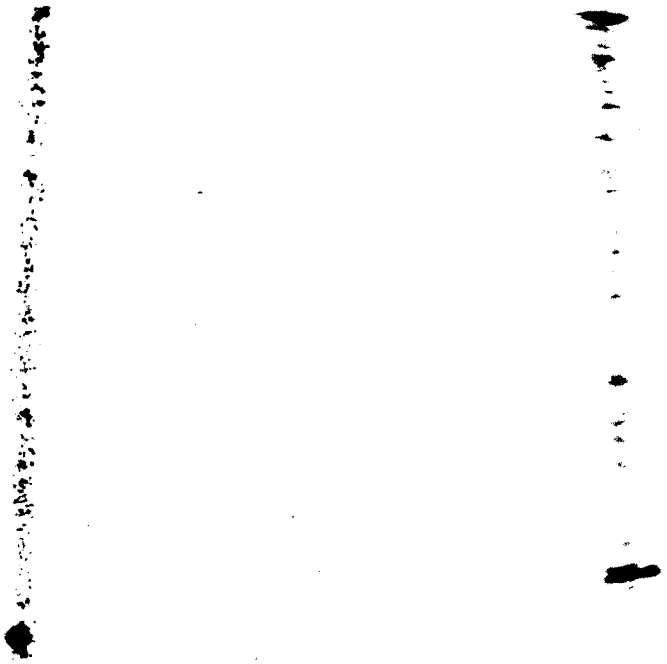

FIG. 4--Streamer track 20 μsec delay in the HV pulse. Diffusion of the primary electrons is seen clearly in the view parallel to $\vec{E}$ (left side picture).

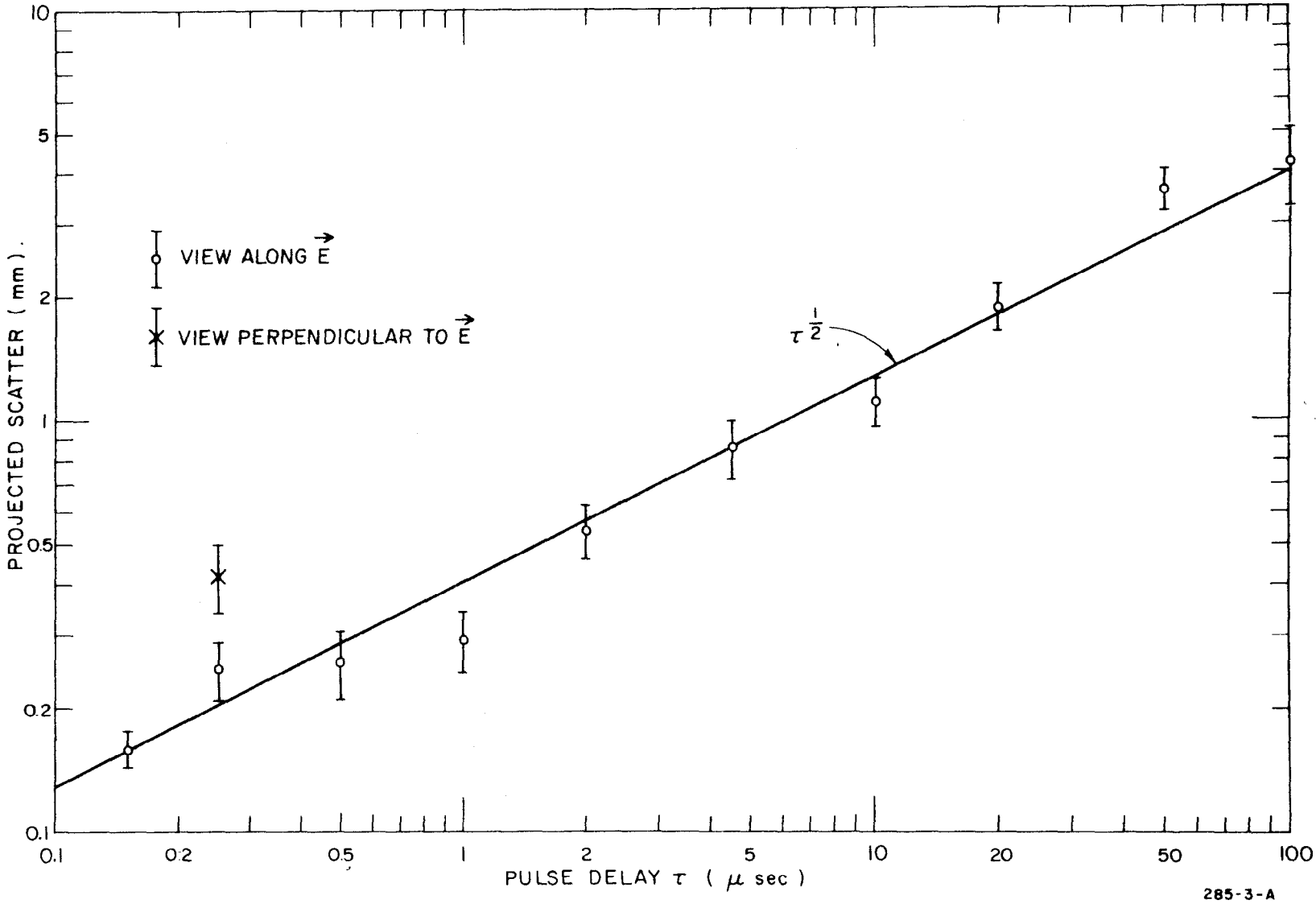

FIG. 5 -- PROJECTED SCATTER (STANDARD DEVIATION) OF STREAMERS FROM PARTICLE TRAJECTORY AS FUNCTION OF TIME DELAY OF HIGH VOLTAGE PULSE.

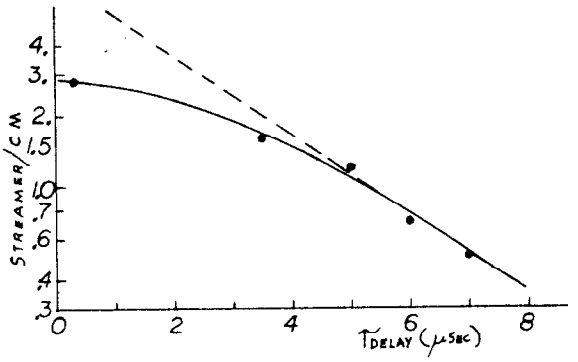

FIG 6(a) STREAMER DENSITY AS A FUNCTION OF PULSE DELAY FOR 14 PPM FREON 12

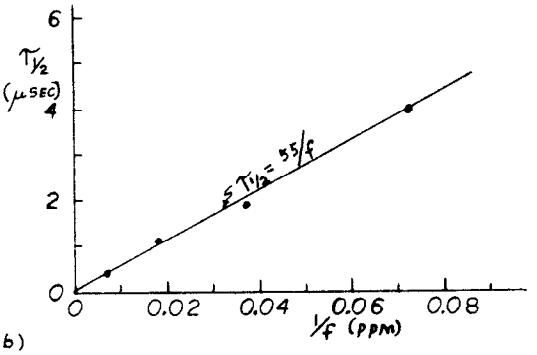

FIG 6(b)

THE TIME AT WHICH THE STREAMER DENSITY HAS DROPPED TO HALF THE T=0 VALUE FOR VARIOUS CONCENTRATIONS, f, OF FREON 12

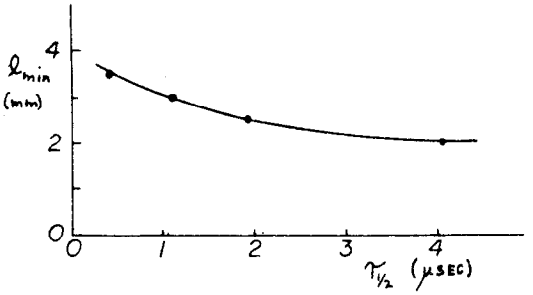

FIG 6(c)

MINIMUM STREAMER LENGTH VISIBLE IN SIDE VIEW (f/1.5, 2475 FILM) FOR VARIOUS MEMORY TIMES

NOTE: FIGS 6.(a,b,c,) SYSTEMATIC ERRORS 20%

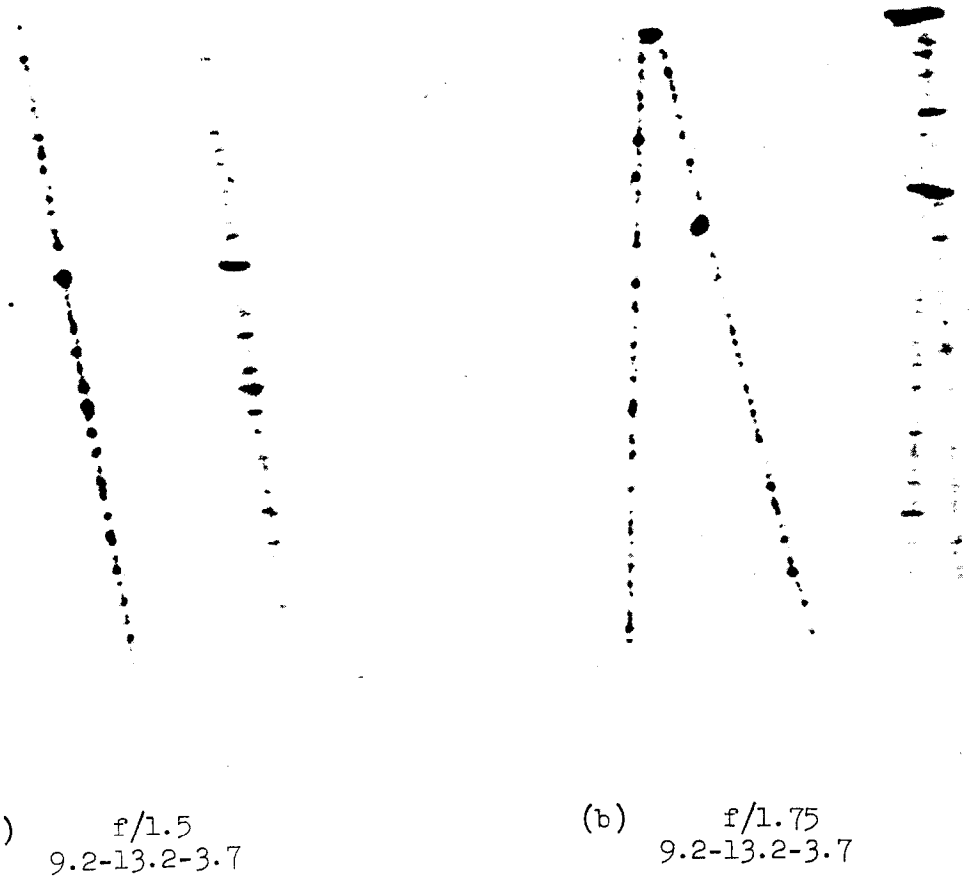

(a) f/1.5
9.2-13.2-3.7

(b) f/1.75
9.2-13.2-3.7

(c) f/2
9.2-13.2-3.7

(d) f/2.4
9.2-13.2-3.7

FIG. 7--Streamer tracks. Direct photography on 2475 film. f-numbers as shown. Numbers below f-number are: pulse width (nsec), pulse height (kV/cm), and streamer width (mm) (average), respectively.

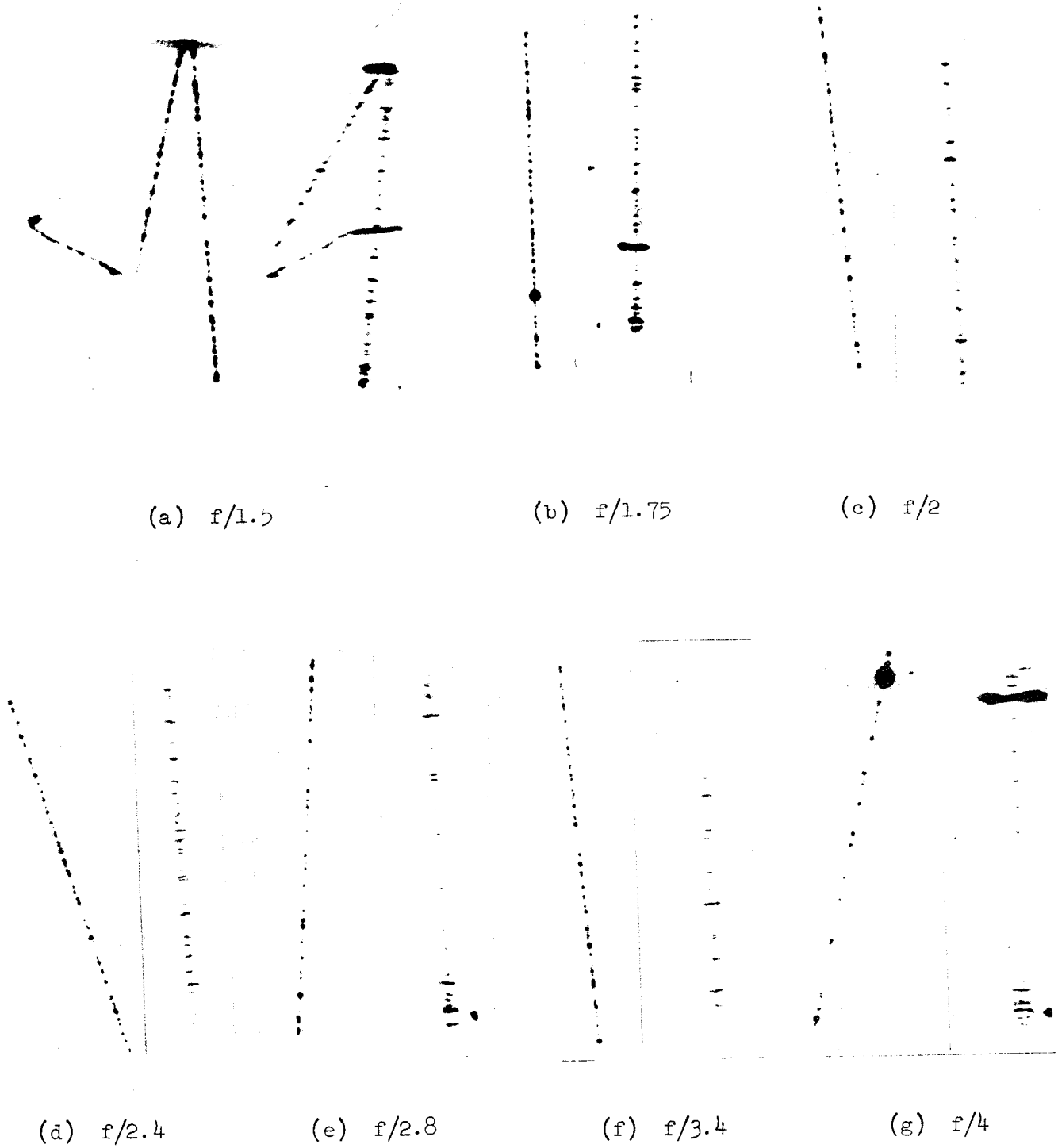

FIG. 8--Streamer tracks. Direct photography on 2475 film. f-numbers as shown f-numbers as shown. Pulse width (nsec), pulse height (kV/cm), and average streamer (mm) width in all pictures are: 6.9, 21.2, 5.3. Note the gradual fading with increasing f-number.

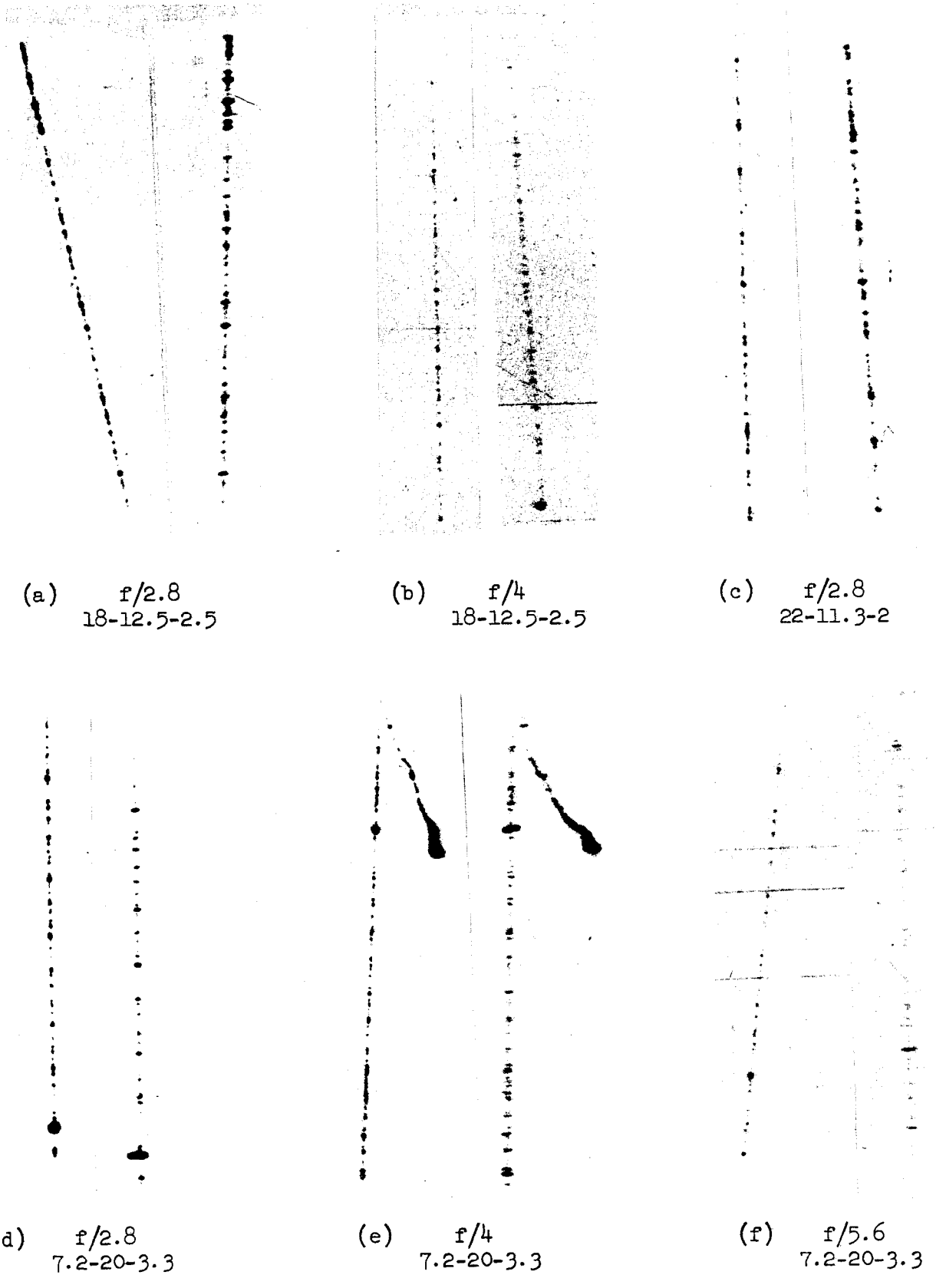

(a) f/2.8 18-12.5-2.5

(b) f/4 18-12.5-2.5

(c) f/2.8 22-11.3-2

(d) f/2.8 7.2-20-3.3

(e) f/4 7.2-20-3.3

(f) f/5.6 7.2-20-3.3

FIG. 9--RCA two-stage image intensifier pictures of cosmic ray streamer tracks. Front lens f-numbers as shown. The numbers below f-number are: pulse width (nsec), pulse height (kV/cm), and streamer length (mm) (average), respectively.

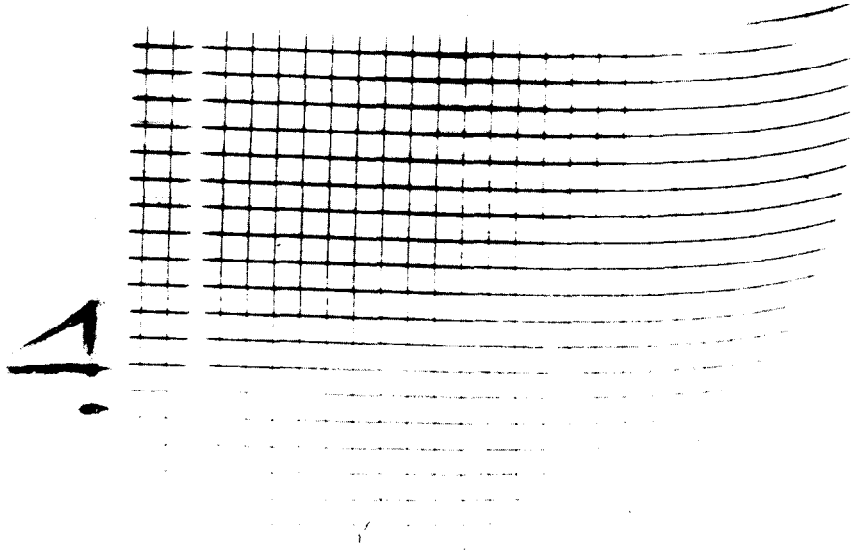

FIG. 10--Typical distortion in one quadrant of RCA two-stage image intensifier. The object is a rectangular grid precision ruled on a lucite plate, and uniformly illuminated through plate edges.

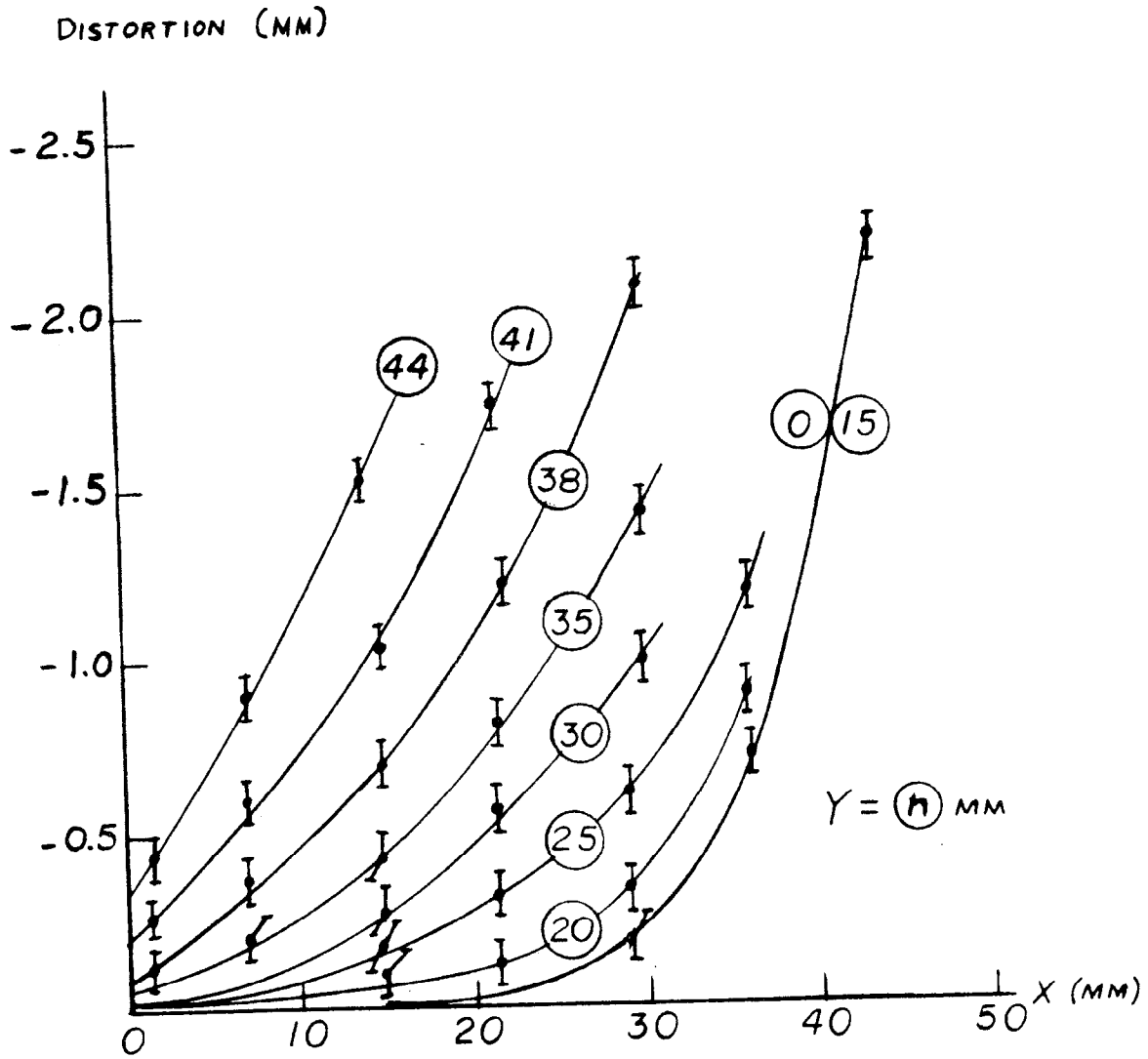

FIG 11 TYPICAL DISTORTION IN ONE QUADRANT OF 2 STAGE RCA IMAGE INTENSIFIER AS FN OF THE UNDISTORTED X, Y CO-ORDINATES. TUBE RADIUS = 45 MM

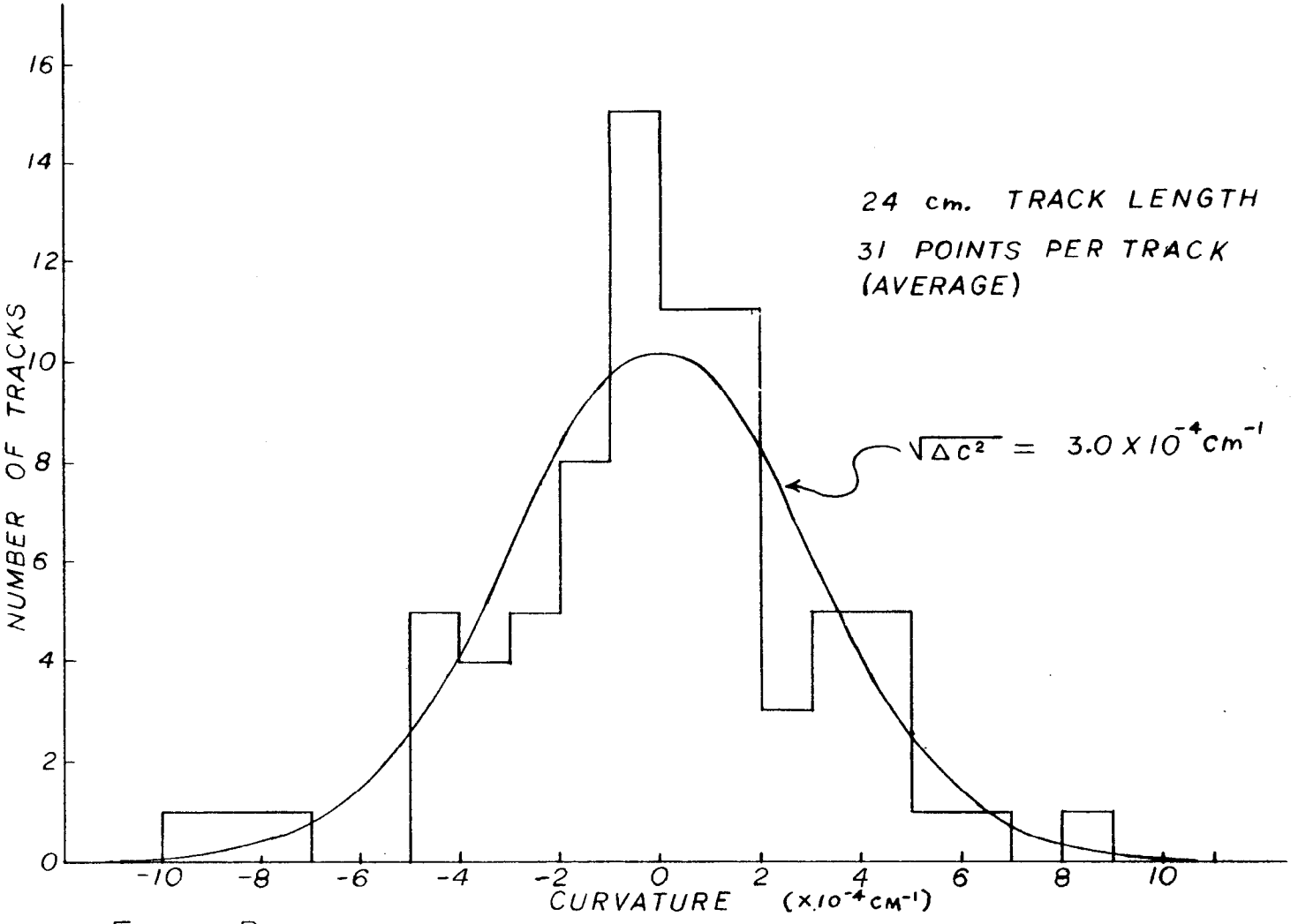

FIG 12 DISTRIBUTION OF CURVATURE MEASUREMENTS FOR 80 STAIGHT TRACKS

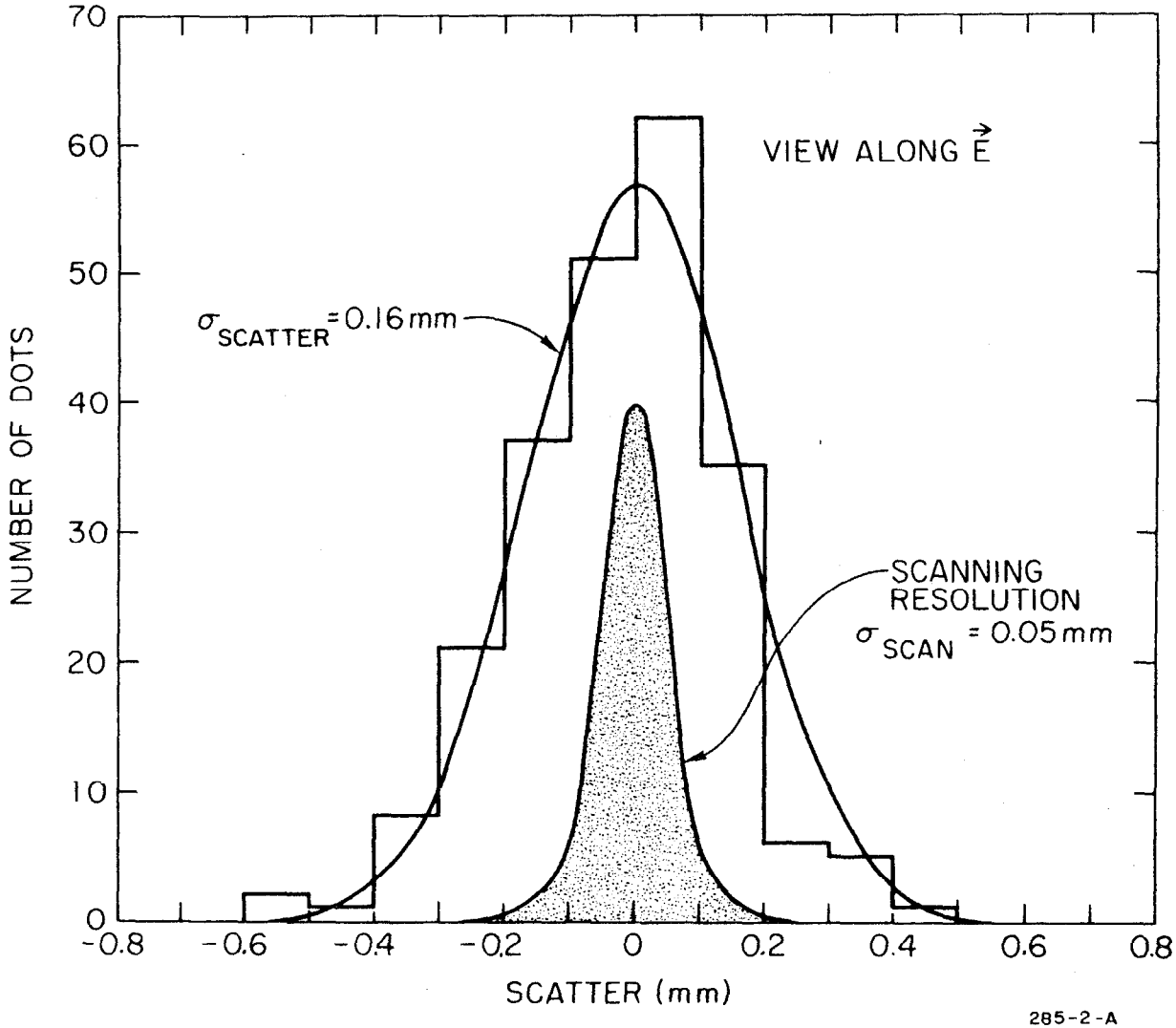

FIG. 13 -- SCATTERING DISTRIBUTION OF STREAMERS FROM PARTICLE TRAJECTORY WITH 0.15 μsec H.V. PULSE DELAY

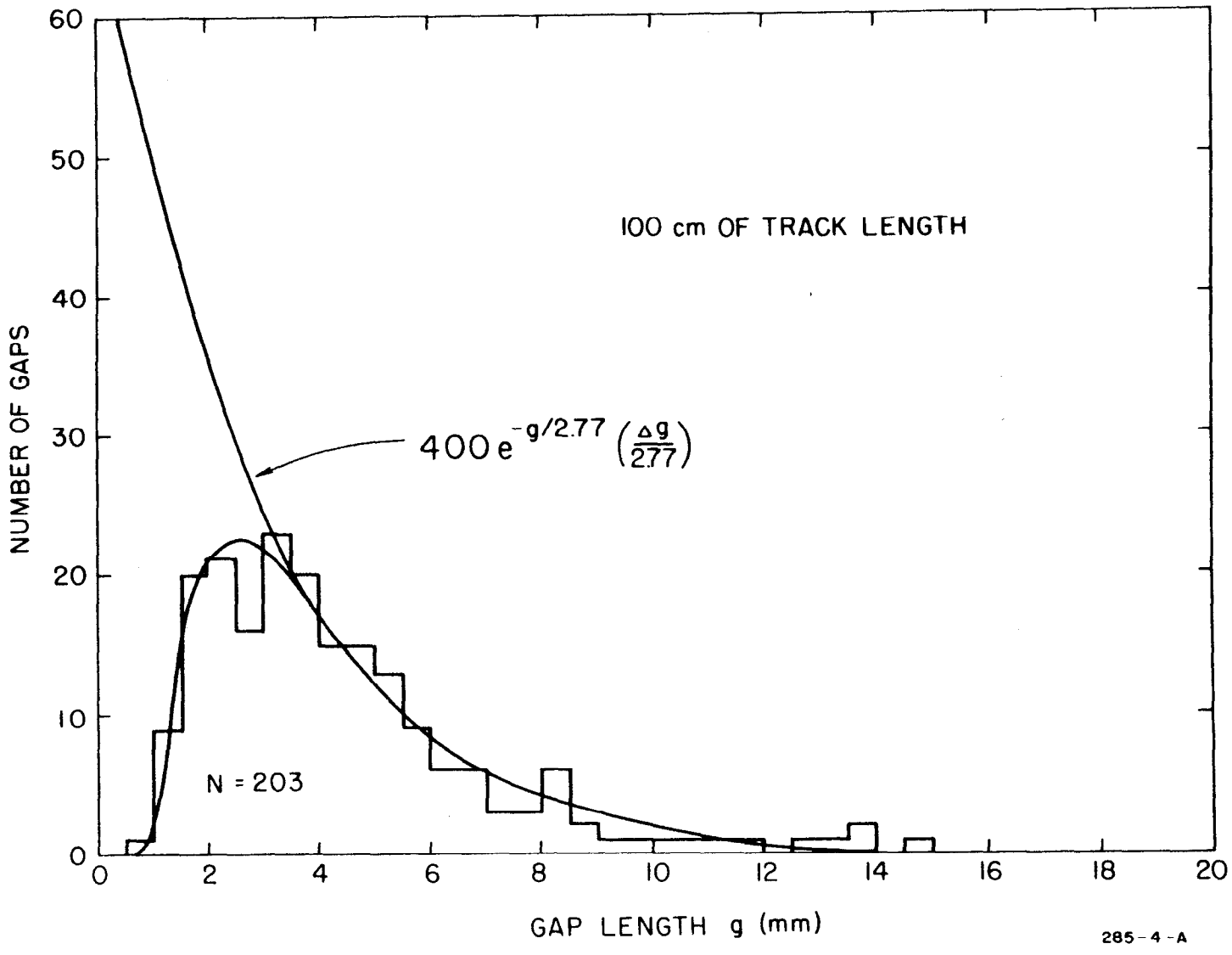

FIG. 14 --STREAMER GAP LENGTH DISTRIBUTION FOR A 0.15 μsec DELAYED H.V. PULSE

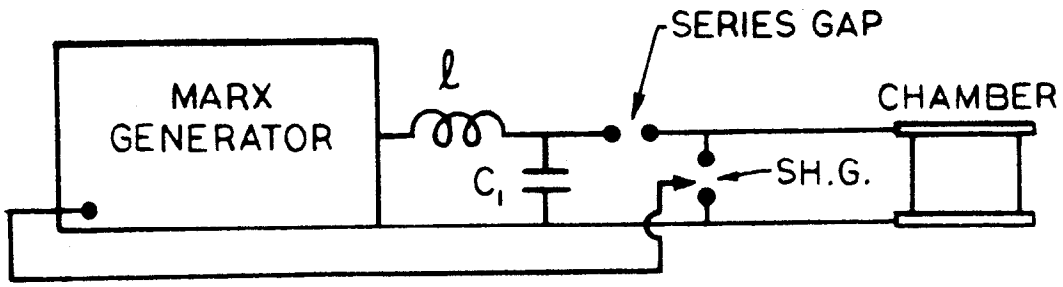

FIG. 15 (a)
SCHEMATIC OF PULSE GENERATOR

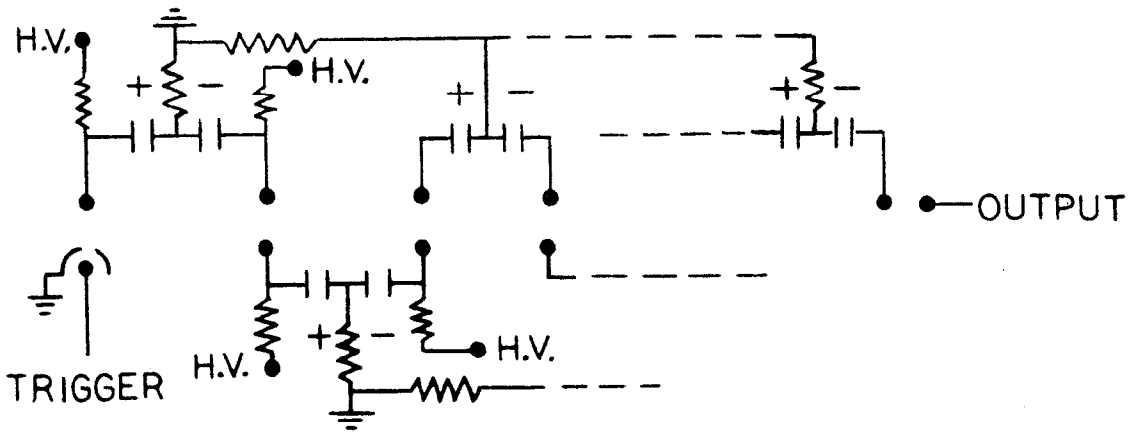

FIG. 15 (b)
SCHEMATIC OF MODIFIED 10 STAGE
(20 CONDENSER) MARX GENERATOR
OUTPUT 800 KV MAX.